Xue, Tianchen; Jokisalo, Juha; Kosonen, Risto

Cost-Effective Control of Hybrid Ground Source Heat Pump (GSHP) System Coupled with District Heating

Published in:
Buildings

DOI:
10.3390/buildings14061724

Published: 08/06/2024

Document Version
Publisher's PDF, also known as Version of record

buildings

MDPI

Article

Cost-Effective Control of Hybrid Ground Source Heat Pump (GSHP) System Coupled with District Heating

Tianchen Xue [1,*], Juha Jokisalo [1] and Risto Kosonen [1,2]

[1] Department of Mechanical Engineering, Aalto University, 02150 Espoo, Finland; juha.jokisalo@aalto.fi (J.J.); risto.kosonen@aalto.fi (R.K.)
[2] College of Urban Construction, Nanjing Tech University, Nanjing 211816, China
* Correspondence: tianchen.xue@aalto.fi

Abstract: Hybrid ground source heat pump systems (GSHP) offer energy flexibility in operation. For hybrid GSHP systems coupled with district heating, limited studies investigated control strategies for reducing system energy costs from the perspective of building owners. This study proposed a cost-effective control strategy for a hybrid GSHP system integrated with district heating, investigating how power limits of district heating/GSHP, COP value for control (COP_{ctrl}), and control time horizon impact the system annual energy cost, CO_2 emissions, and long-term borehole heat exchanger system performance. The simulations were performed using the dynamic building simulation tool IDA ICE 4.8. The results indicate that to realize both the energy cost savings and the long-term operation safety, it is essential to limit the heating power of district heating/GSHP and select an appropriate COP_{ctrl}. The control time horizon insignificantly affected the annual energy cost and long-term borehole heat exchanger system performance. The recommended COP_{ctrl} was 3.6, which is near the GSHP seasonal performance factor. Eventually, the cost-effective control reduced the system's annual energy cost by 2.2% compared to the GSHP-prioritized control. However, the proposed control increased the CO_2 emissions of the hybrid GSHP system due to the higher CO_2 emissions from district heating.

Keywords: hybrid ground source heat pump; district heating; borehole free cooling; cost-effective control

Citation: Xue, T.; Jokisalo, J.; Kosonen, R. Cost-Effective Control of Hybrid Ground Source Heat Pump (GSHP) System Coupled with District Heating. *Buildings* **2024**, *14*, 1724. https://doi.org/10.3390/buildings14061724

Academic Editor: Antonio Caggiano

Received: 25 April 2024
Revised: 28 May 2024
Accepted: 6 June 2024
Published: 8 June 2024

1. Introduction

The buildings sector accounts for nearly 30% of global energy consumption and 26% of global operational-related CO_2 emissions [1]. Decarbonizing the global buildings sector is consequently essential to averting severe climate change. In order to achieve the targets of the Paris Agreement, all new buildings must be net-zero carbon in operation by 2030, and all existing and new buildings must be net-zero carbon across the whole life cycle by 2050 [2]. In this context, ground source heat pumps (GSHPs) are potentially effective solutions for decarbonizing energy for the heating and cooling of buildings.

GSHP system can provide high-efficient heating and can be adaptable to various environments [3]. Moreover, the system can generate borehole free cooling along with high-temperature cooling terminal units, such as radiant panels and chilled beams with an inlet water temperature ranging from 16 to 18 °C in summer. Due to the advantages, the GSHP market in Europe experienced an expansion in the last few years [4]. Finland, as one of the northernmost countries, has utilized the GSHP technology extensively [5]. According to the Finnish Heat Pump Association, annual sales of large-scale GSHPs (with a maximum heating capacity of over 26 kW) exceeded 2000 units in 2023 [6].

GSHP efficiently transfers heat to and from the ground through multiple borehole heat exchangers, composing what is commonly referred to as a borehole field for heating or cooling purposes. Appropriate design of the borehole field is crucial to ensure the sustainability of the whole GSHP system. However, designing borehole fields still faces several challenges in Finland. As the climate in Finland falls under the Df category (cold,

no dry season) in the Köppen Geiger climate classification [7], most buildings are heating-dominant. In the case of using GSHP, the borehole field needs to handle more heating than cooling load. On the one hand, an undersized borehole field would result in an overcooled ground, leading to deterioration of the coefficient of performance (COP) of the system and even damage to the brine heat exchangers due to the volumetric expansion of the groundwater in boreholes [8]. On the other hand, an oversized borehole field would sharply increase the investment expenses, rendering the system economically unfeasible. Therefore, the optimal design of the borehole field needs to consider both the ground temperature limit and investment cost. Detailed reviews of the borehole field design studies have been conducted by several researchers [9–11].

A potential solution to solve the challenges is to install an auxiliary heating system to cover the peak heating load and use the GSHP for the base heating load, composing a hybrid GSHP system [12]. The auxiliary heating source can be solar thermal collectors, electricity boilers, or even district heating. Even though the hybridization of the system can significantly reduce the drilling cost for longer boreholes, the presence of multiple heating sources complicates the control of hybrid GSHP systems. Without optimal control, the anticipated energy savings from the hybrid GSHP system may be constrained. Therefore, implementing smart control for hybrid GSHP systems is crucial to ensure optimal performance, particularly when considering the characteristics of the backup heating source.

The backup heating sources can be generally classified as stable and unstable heating sources. Solar energy exemplifies an unstable heating source, given its sensitivity to unpredictable weather conditions. The hybrid system where the GSHP is coupled to solar collectors is the so-called solar-assisted GSHP system [13]. In this system, solar collectors can produce domestic hot water (DHW) and space heating for the building [13]. In addition, the solar energy can be used to charge the ground [14,15]. Injecting solar heat into the ground can increase the COP of the heat pump but may also increase the pumping energy and reduce the solar fraction [16]. In the case of borehole free cooling, the ground charging time needs to be controlled according to the operating limit of the borehole heat exchanger outlet temperature [16]. Due to the multiple usage ways of solar energy, solar-assisted GSHP systems often use rule-based control methods, which establish specific operational modes for the system. For example, Reda [16] investigated different control strategies of a solar-assisted GSHP for a building located in Helsinki, Finland. He compared three operational modes: (1) solar heat used for charging the ground all the time, (2) solar heat used for charging the ground from November to February and to produce DHW and space heating for the rest of the year, and (3) solar heat used primarily for supplying DHW and space heating and secondarily for charging the ground. The results showed the third operational mode is the optimal one for short and long boreholes in terms of high seasonal system efficiency.

Apart from solar energy, stable backup heating sources like electric boilers and district heating are widely used in hybrid GSHP systems. These systems can utilize advanced model-based control strategies to optimize load distribution among multiple heating sources, considering energy price differences and system efficiencies among different supply systems. In previous studies, model-based control methods, such as dynamic programming control, model predictive control (MPC), and linear optimal control, have been used for the optimal load distribution [17]. In these methods, the objective of the control is to minimize the cost function over a certain period subject to specific constraints. For dynamic programming control and linear optimal control, it is even possible to apply a constraint of zero thermal imbalance to the ground during the whole control period.

The optimal load distribution can also be conducted through a rule-based control method. Atam et al. [18] derived a specific criterion denoted as '*r*' from the cost function of a hybrid GSHP system, incorporating a GSHP, a gas boiler, a passive cooler, and an active chiller. The criterion is related to time-dependent energy prices, heat pump COP, and boiler efficiency. This criterion can be used for determining whether to use the GSHP or the boiler. Based on observations, it can be inferred that the determined criterion 'r' may be

incorporated into a rule-based control strategy, obviating the necessity for a model-based control algorithm. However, this type of control method requires additional adjustments to the determined criterion or other control rules to realize the temperature constraints of brine temperature. For example, Puttige et al. [19] added one penalty variable to the determined criterion to minimize the annual operational cost of heating and cooling by ensuring a balanced operation of the ground.

The primary challenge of cost optimization lies in the prediction of GSHP's COP. Generally, the heat pump COP hinges on the GSHP operational conditions, such as the inlet temperatures of the working fluids into the evaporator and condenser and the mass flow rates through the evaporator and condenser. For modulating GSHPs, COP is further affected by the partial load condition of the heat pump, which is controlled by a frequency inverter. The formulation of the heat pump COP can affect the control optimization result of the hybrid GSHP system.

Many studies have investigated different formulations of the heat pump COP for control optimization in hybrid GSHPs. Verhelst [20] applied a linear MPC method to optimize the operation of a hybrid GSHP system comprising a heat pump, a borehole field, a gas boiler, and a chiller. The objective is to maximize the thermal comfort, minimize energy costs, and realize the long-term sustainability of the ground. He compared the nonconvex optimization problem caused by the temperature-dependent COP with the convex optimization problem induced by a simplified constant COP based on the weekly time-step case. The comparative study revealed almost no difference between simplified and accurate COP representations when the cost function penalized power peaks. Weeratunge et al. [21] developed an MPC using a mixed integer linear programming approach to optimize the operation cost for a solar-assisted GSHP system coupled with thermal storage and electricity heater under dynamic electricity prices. The formulation of COP of a heat pump for a given flow rate is linear to the entering water temperature of the heat pump. They compare the MPC with a setpoint control. The results showed the operational cost of the solar-assisted GSHP system was reduced by 7.8% by MPC compared to the setpoint-based control. Atam et al. [22] proposed a convexification method for nonconvex optimal and model predictive control problems in HVAC systems. The method was tested on a hybrid GSHP case where the heat pump COP is calculated as a linear function of the fluid temperature. The proposed convexified optimal control was compared to a dynamic programming control for the total energy cost minimization of the hybrid GSHP system. The results of the convexified optimal control were similar to those obtained by using dynamic programming. Atam et al. [18] also conducted a detailed simulation-based analysis of three different control approaches, including a prediction-based dynamic programming control, a nonlinear model predictive control, and a linear optimal control, for minimizing the energy consumption of a hybrid GSHP system coupled to a gas boiler and a chiller. The results showed that the energy consumption minimization results by using nonlinear MPC and the linear optimal control assuming constant heat pump COP values were very close to the results by using the dynamic programming control with less than 10% deviation. Figueroa et al. [23] analyzed four different MPC modeling strategies, considering whether to use a complicated formulation of the COP and whether to use a complex borehole field. They found that using a constant COP can cause a bang–bang behavior (completely on and off) of the heat pump. In contrast, accurate modeling of the COP dependent on sink and source temperatures, variable mass flow rates, and the modulation level can realize a smoother operation of the heat pump. Furthermore, accurate COP predictions can help MPC realize more savings under a higher electricity-to-gas price ratio. The total energy cost was saved by 0.5%, 1.9%, and 2.7% for the low, average, and high electricity-to-gas price ratios, respectively.

In contrast to research regarding hybrid GSHP systems with boilers, there is relatively limited work on control optimization for hybrid GSHP systems integrating district heating. The characteristic of the district heating tariff differentiates the control optimization problem from the electricity boiler. In Finland, the district heating tariff contains two parts: the

power fee determined by the peak district heating power used during the whole year and the energy fee based on energy consumption. This characteristic of the district heating tariff introduces more complexity to the control of the hybrid heating system.

So far, only a few studies have tackled control optimization in hybrid GSHP systems coupled with district heating. Puttige et al. [19] presented a rule-based control method to minimize the annual operational cost of heating and cooling for a hybrid GSHP system coupled with district heating and cooling. The GSHP system model was developed by using both an analytical model and an artificial neural network. However, the new control method was developed to save energy costs only from the perspective of the energy provider. The heating power limits of GSHP or district heating and power fees were not considered in the analysis. In addition, the control time horizon in their proposed control was only one hour, which means the price comparison was only carried out for the next one hour. The effect of a longer control time horizon was not considered. Gustafsson and Rönnqvist [24] used mixed integer linear programming (MLIP) models to minimize the life cycle cost of a hybrid heating system consisting of the GSHP, district heating, and gas boiler for building owners. The results suggested that the mixed integer linear programming was able to adequately address both the district heating and the electricity tariffs. Nevertheless, in their optimization work, the electricity price and heat pump COP were both set as constant for the whole year, which neglected the effects of the dynamic price difference and justification of the assumed heat pump COP.

Therefore, based on the authors' best knowledge, below are the following research gaps:

- There are limited studies focused on minimizing energy costs in hybrid GSHP systems integrated with district heating, considering the heating power limits of GSHP and district heating on the energy cost for building owners.
- The effects of heat pump COP value and control time horizon in cost-effective controls have not been investigated in hybrid GSHP systems integrated with district heating.

The study aims to investigate several control parameters of a cost-effective control strategy for reducing the total energy cost of a hybrid GSHP coupled with district heating from the perspective of building owners. The studied parameters include the heating power limits of GSHP/district heating, heat pump COP value for control, and control time horizon. The hybrid GSHP system was modeled and simulated by IDA Indoor Climate and Energy (IDA ICE) 4.8. Based on the model, a rule-based control strategy was developed to minimize the energy cost for the hybrid GSHP system. The effects of studied parameters on the short-term hybrid GSHP system performance, energy cost, CO_2 emissions, and long-term brine temperature behavior were analyzed.

2. Methodology

2.1. Building Simulation Tool

The studied building and hybrid GSHP system was simulated in the building simulation tool IDA ICE 4.8 [25], which is a dynamic multizone simulation software for the studies of thermal indoor climate and building energy consumption. It is able to model detailed building characteristics and different technical systems, such as heat pumps and borehole thermal storage systems. The software supports simulations with variable time steps. Its reliability has been proved against EN 15255−2007 and EN 15265−2007 standards [26].

To accelerate the computational process, the borehole field model was separated from the combined model of the building and hybrid GSHP system. These two models were connected via two interfaces to exchange essential data, such as brine flow rate, brine pressures, and brine temperatures, at each computational step. Both models were simulated concurrently during the simulation process. The borehole field model has already been validated in a prior study by Xue et al. [27].

2.2. Description of Simulation Process

A flow chart of the simulation process is shown in Figure 1. The developed control algorithm (See Section 2.5) receives the hourly electricity price and monthly district heating

price and then generates control signals to determine the primary and backup heating sources in the hybrid GSHP system. After that, the control signals will be sent to the IDA ICE. Additionally, the energy price, the weather data, and other key parameters are inputted into the IDA ICE. Eventually, the IDA ICE software will conduct the simulation and generate the results.

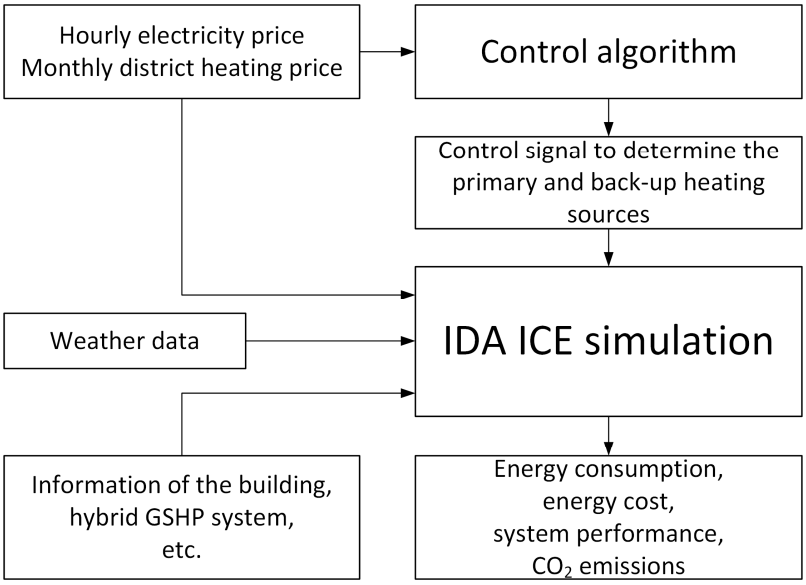

Figure 1. Flow chart of simulation process.

2.3. Building Description

The studied building is an educational building complex in Espoo, Finland. The building has an irregular shape. It consists of five floors and several functioning spaces such as office rooms, educational spaces, restaurants, stores, supermarkets, and a metro station. The net floor area of the building is 47,500 m^2. The building was constructed from 2018 to 2019. It has been fully taken into use since June 2019.

The original building geometry was simplified into a single-story and rectangular design. The room height was set as 4.6 m. The zoning was also simplified into a five-zone layout. To obtain the actual net floor area, the final geometry of the building was enlarged by a zone multiplier of 18.3. Figure 2 shows the geometry of the simplified building model. Key input parameters, such as the building's geometry, U-values of the envelope, and window properties, are given in Table 1. The building envelope and windows are designed according to the Finnish building code [28].

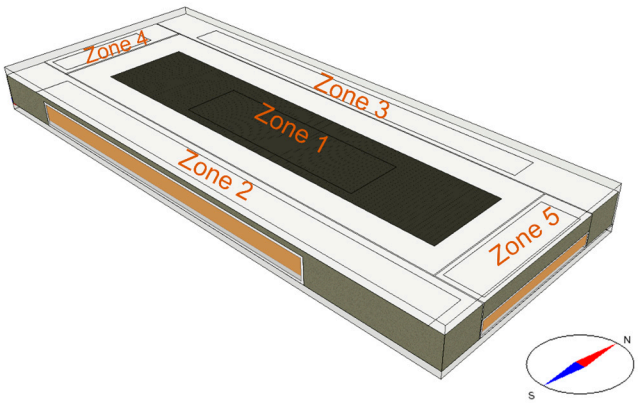

Figure 2. Geometry of the simplified building model.

Table 1. Overview of the building model parameters.

Parameters		Value
Heated net floor area, m^2		47,500
Envelope area, m^2		51,224
Window to envelope ratio, %		17.3
U-value, W/m^2K	External walls	0.17
	Roof	0.09
	Ground slab	0.18
	Windows	0.6
Window glazing properties	Total solar heat transmittance	0.49
	Direct solar transmittance	0.41
Window opening		Never open
Air tightness q_{50}, m^3/hm^2		2 (at 50 kPa)
Solar shading	Internal shading	Interior roll (Solar radiation > 100 W/m^2)
	External shading	None

A hydronic four-pipe radiant ceiling panel system is used for distributing space heating and cooling energy. The design outdoor temperature and indoor air heating setpoint temperature are −26 °C and 21 °C. The design indoor air cooling setpoint is 25 °C. The dimensioning supply/return water temperatures for space heating are 49/30 °C. The supply water temperature for space heating is adjusted according to the variation in outdoor air temperature. The dimensioning supply/return water temperatures for space cooling are 15/18 °C.

The internal heat gains from the occupants were determined based on an activity level of 1.0 MET with a clothing of 0.85 ± 0.25 clo. Due to the multiple functions of the building, different occupancy densities and heat gains from lighting and equipment were set for the five zones in the simplified building model. The settings of occupancy density and internal heat gains from lighting and equipment are shown in Table 2. The heating energy demand for domestic hot water (DHW) was set as 7.5 kWh/m^2a.

Table 2. Internal heat gains.

Parameters	Zones 1−3	Zones 4−5
Occupants	Occupancy density 0.13 $1/m^2$	Occupancy density 0.86 $1/m^2$
Lighting	Average gain 8.0 W/m^2	Average gain 19.6 W/m^2
Equipment	Average gain 5.0 W/m^2	Average gain 11.2 W/m^2

A mechanical balanced ventilation system with heat recovery is installed in the building. In the model, the ventilation was simulated with two air handling units (AHUs). The AHU heating is designed with dimensioning supply/return water temperatures set at 45/30 °C. The AHU heating supply water temperature is dynamically adjusted based on outdoor air temperature variations. The AHU cooling is designed with dimensioning supply/return water temperatures of 10/16 °C. The supply air temperature varies between 16 and 18 °C. The detailed settings of air flow rates are given in Table 3. The fan operates on weekdays at maximum speed from 7:00 to 19:00 and at 20% speed from 23:00 to 4:00. Between 4:00 and 7:00, the fan speed gradually increases, while from 17:00 to 22:00, it gradually decreases.

Table 3. Ventilation air flow rates.

Zone	Supply and Exhaust Air Flow Rates (L/sm^2)
Zone 1	3.5 (7:00−19:00) 0.7−3.5 (4:00−7:00, 19:00−23:00) 0.7 (23:00−4:00)
Zone 2−3	2.0 (7:00−19:00) 0.4−2.0 (4:00−7:00, 19:00−23:00) 0.4 (23:00−4:00)
Zone 4−5	2.5 (7:00−19:00) 0.5−2.5 (4:00−7:00, 19:00−23:00) 0.5 (23:00−4:00)

2.4. Hybrid GSHP System

A simplified schematic of the hybrid GSHP system model is shown in Figure 3. The hybrid GSHP system consists of a heat pump, a borehole field, a district heating substation, chiller, and water storage tanks. The borehole field is connected in series to the heat pump evaporator and heat exchanger HX3. The hot water storage tank provides the hot water for the heating network. It was heated jointly by the heat pump condenser and heat exchanger HX2 in the district heating substation. The other heat exchanger (HX1) in the district heating substation is used for producing DHW. The cold water storage tank connected to the evaporator of the chiller and heat exchanger HX3 supplies cold water to the cooling network.

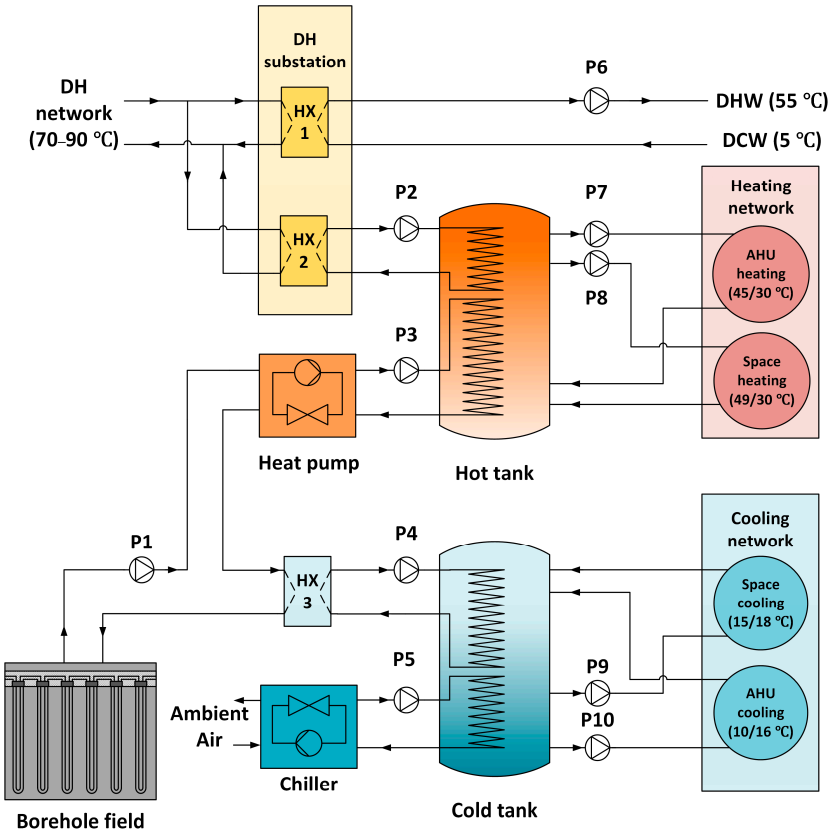

Figure 3. Simplified schematic of the hybrid GSHP system model.

There are nine heat pump units in the hybrid GSHP system. The total heating capacity of heat pumps is 790 kW with a COP of 3.94 at rating conditions of 35/0 °C. During the modeling phase, a single brine-to-brine heat pump model was used to represent the nine heat pump units. The heat pump model comprises heat exchanger models based on the

NTU method, and a compressor model based on the performance descriptive correlation. More detailed descriptions of the IDA ICE heat pump model were outlined in the study by Niemelä et al. [29].

The district heating substation provides backup heating and DHW with an efficiency of 97% in the model. The design power of the backup district heating is 1680 kW. The district heating supply temperature is controlled between 70 °C and 90 °C according to the outdoor temperature.

The air-cooled chiller provides backup cooling to the cooling network with an efficiency ratio (EER) of 3.04. The nominal cooling capacity of an air-cooled chiller is 1300 kW.

The borehole field was modeled through the IDA ICE ground heat exchanger (IDA ICE GHX) module developed by means of the finite difference method. The boreholes are drilled in the granite-dominated bedrock. On top of the bedrock covers 10 m of soil. Each borehole is 310 m deep with a diameter of 115 mm. Each borehole is filled with groundwater. The borehole heat exchangers are plastic single U-tubes filled with a 28% ethanol–water mixture. In the model, the original irregular borehole field layout (see Figure 4a) was simplified to a double-symmetry layout (see Figure 4b). The final simulation result for the borehole field was produced by replicating the simulation results of the 21 boreholes shown in Figure 4b as red dots. The borehole field models were described in the previous work [27] and validated against the measured brine temperature data. The input parameters shown in Table 4 were used in the simplified borehole field model.

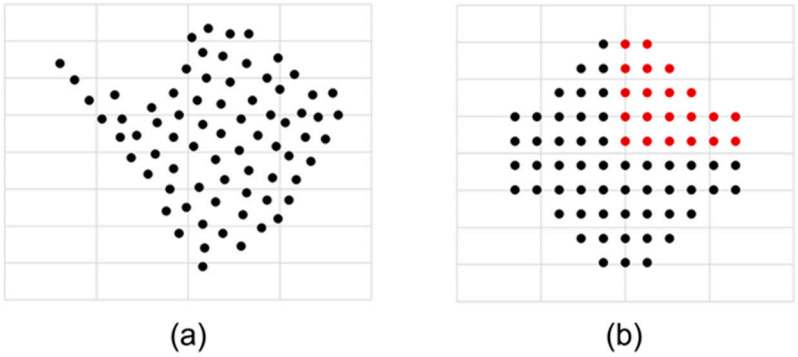

Figure 4. Borehole field layouts, (**a**) original layout, and (**b**) simplified layout.

Table 4. Input parameters for borehole field model.

Descriptive Parameters	Value
Number of boreholes, pcs	74
Equivalent spacing between boreholes, m	13.1
Borehole average depth, m	310
Borehole diameter, mm	115
U-pipe outer diameter, mm	40
U-pipe wall thickness, mm	2.4
U-pipe thermal conductivity, W/mK	0.42
Brine freezing point, °C	−18.5
Brine thermal conductivity, W/mK	0.417
Brine density, kg/m^3	961
Brine specific heat capacity, J/kgK	4243
Brine dynamic viscosity, Pa·s	0.00328
Groundwater effective thermal conductivity, W/mK	1.6 (considering convection)
Groundwater density, kg/m^3	1000
Groundwater specific heat capacity, J/kgK	4200
Bedrock thermal conductivity, W/mK	3.3
Bedrock density, kg/m^3	2500

Table 4. *Cont.*

Descriptive Parameters	Value
Bedrock specific heat capacity, J/kgK	725
Geothermal temperature gradient, °C/m	0.0119
Undisturbed ground temperature, °C	8.7
Effective borehole thermal resistance, mK/W	0.095 (0.0977 for heat injection)

The nonideal storage tank model was used for modeling the hot and cold storage tanks. The validity of the tank model was proved by Alimohammadisagvand et al. [30]. The hot storage tank model was set with a volume of 5 m^3 and a height of 2.2 m. The cold storage tank model was set with a volume of 3 m^3 and a height of 2.0 m. Both storage tanks have 8 layers from bottom to top. Two temperature sensors were set at the top of the hot storage tank and the bottom of the cold storage tank, respectively. The temperature setpoint of the top layer of the hot storage tank ($T_{set,\,HSL}$) was set as 2 °C higher than the maximum supply water setpoint for the AHU and space heating. The temperature setpoint of the bottom layer of the cold storage tank ($T_{set,\,HSL}$) was set as 2 °C lower than the minimum supply water setpoint for the AHU and space cooling.

2.5. Operation of the Heating and Cooling System

The heating and cooling system was operated with different indoor air setpoints and control strategies for the hybrid GSHP system in two operational periods. Until the end of August 2022, the building was operated with the indoor air heating setpoint of 21 °C and cooling setpoint of 25 °C. A GSHP-prioritized control strategy was used for controlling the hybrid GSHP system. Since September 2022, the new indoor air setpoints and the new control strategy for the hybrid GSHP system have been used. The indoor air heating setpoint of 21 °C remained, while the indoor air cooling setpoint was reduced to 23 °C to increase the use of borehole free cooling. Moreover, a cost-effective control strategy was implemented in the hybrid GSHP system.

2.5.1. GSHP-Prioritized Control Strategy

The GSHP-prioritized control strategy uses the GSHP to cover the base heating load. The district heating is used as backup heating. The backup heating will be activated if the GSHP is operating at maximum power and the measured water temperature of the hot storage tank $T_{mea,\,HSL}$ is lower than the hot storage tank setpoint $T_{set,\,HSL}$.

For cooling purposes, the system prioritizes the usage of free cooling energy from the borehole field. The temperature of the free cooling water in the cold storage tank is determined by the outlet brine temperature from the borehole heat exchangers. The brine temperature difference between the inlet and outlet of the borehole heat exchanger is regulated to 5 °C. The chiller will start working if the brine pump P1 in Figure 3 works at the maximum mass flow rate and the measured water temperature from the bottom layer of the cold storage tank $T_{mea,\,CSL}$ is higher than the cold storage tank setpoint $T_{set,\,CST}$.

2.5.2. Cost-Effective Control Strategy

In the cost-effective control strategy, the operation in the transition and cooling seasons from May to September remained the same as the GSHP-prioritized control. However, the operation in the heating season from October to April was optimized by changing the heating load distribution between the GSHP and the district heating network. The objective is to reduce the annual energy cost from the point of view of the building owner. Generally, if one heating source presents the hourly specific heating cost (€/MWh) consecutively lower in the control time horizon k, it will be selected as the primary heating source in the next one hour. Once the primary heating source is determined, the other heating source is chosen for backup heating. The backup heating will still be activated if the primary heating equipment cannot provide sufficient heat to the hot storage tank.

The heating price signal C and the primary heating source signal CS were used for determining the primary heating source in the optimization period. The heating price signal C, which is 1 representing a lower specific heating cost by using GSHP and 0 representing a lower specific heating cost by using district heating, is determined for each hour τ based on Equation (1). The primary heating source signal CS, which is 1, indicating that the GSHP is used as the primary heating source, and 0, indicating that the district heating is used as the primary heating source, will be determined for the next hour based on Equations (2) and (3).

$$C(\tau) = \begin{cases} 1, if\ \frac{c_e(\tau)}{COP_{ctrl}} \leq \frac{c_d(\tau)}{\eta_{dh}} \\ 0, otherwise \end{cases}, \tau = 1, 2, \ldots, n \quad (1)$$

$$CS(\tau) = C(\tau), \tau = 1 \quad (2)$$

$$CS(\tau) = \begin{cases} 1, if \sum_{i+1}^{i+k} C(\tau) = k \\ 0, if \sum_{i+1}^{i+k} C(\tau) = 0 \\ CS(\tau - 1), otherwise \end{cases}, \tau = 2, 3, \ldots, n \quad (3)$$

where c_e is the hourly electricity price, €/MWh; COP_{ctrl} is the heat pump COP value for control; c_d is the monthly district heating price, €/MWh; η_{dh} is the efficiency of district heating substation; C is the heating price signal; CS is the primary heating source signal; k is the control time horizon, h; and τ is the serial number of hours of the simulation time.

2.6. Evaluation of Short-Term and Long-Term Performances of Hybrid GSHP System

The performance of the hybrid GSHP system is evaluated over a short-term period of 1 year and a long-term period of 30 years. The short-term hybrid GSHP system performance is evaluated via the following key performance indicators: GSHP operational time ratio (TR), GSHP heating energy ratio (HR), ground thermal imbalance ratio (IR), and seasonal performance factor (SPF). The definitions of the key performance indicators are shown as follows:

$$TR = \frac{T_{GSHP}}{8760} \times 100\% \quad (4)$$

$$HR = \frac{Q_{cond}}{Q_{heat,tot}} \times 100\% \quad (5)$$

$$IR = \frac{Q_{ext} - Q_{inj}}{Q_{max}} \times 100\% \quad (6)$$

$$SPF = \frac{Q_{cond}}{Q_{comp}} \times 100\% \quad (7)$$

where T_{GSHP} is the total GSHP operating hours in a given year; Q_{cond} is the total condenser heat of the GSHP in a given year, kWh; Q_{comp} is the total electricity consumption by the compressor of the GSHP in a given year, kWh; $Q_{heat,\ tot}$ is the total heating energy for space and AHU heating in a given year, kWh; Q_{ext} is the total heat extraction from the ground in a given year, kWh; Q_{inj} is the total heat injection to the ground in a given year, kWh; and Q_{max} is the maximum value between Q_{ext} and Q_{inj}.

The long-term performance of the borehole field is evaluated via the mean brine temperature T_f calculated by Equation (8).

$$T_f = \frac{T_{in} + T_{out}}{2} \quad (8)$$

where T_f is the mean brine temperature, °C; T_{in} is the borehole field inlet brine temperature, °C; and T_{out} is the borehole field outlet brine temperature, °C.

2.7. Energy Tariffs

The energy cost calculation comprises the cost for the total electricity and the backup district heating in the hybrid GSHP system. The district heating cost for DHW is not considered, as the DHW generation is not impacted by the system control strategy. The electricity cost includes the energy and power costs. The electricity energy cost was calculated based on the hourly electricity price and the hourly electricity consumption in the hybrid GSHP system. The hourly electricity price consists of three parts: the real-time electricity price from Nord Pool [31], the marginal price, and distribution fees. The electricity power cost was calculated based on the monthly basic fee and power fee for the monthly peak electricity power. The district heating cost also includes the energy and power costs. The district heating energy cost was calculated by the monthly average district heating price from a local district heating and the monthly district heating consumption for backup heating. The district heating power cost is calculated based on the used power and the reserved power. The used power is the average of three hourly peak district heating powers during the year. The reserved power is the difference between the design power and the used power. Table 5 gives the detailed distribution and power fees including all taxes. Figure 5 shows the hourly electricity price and monthly district heating price (including all taxes) in the first year using cost-effective control.

Table 5. Distribution and power fees (including all taxes).

Item	Distribution and Power Fees	
Electricity	Marginal price	0.236 c/kWh
	Distribution fee	4.46 c/kWh
	Basic fee	333.56 €/month
	Power fee	2.17 €/kW, month
District heating	Used power fee	6.2 €/kW, month
	Reserved power fee	1.03 €/kW, month

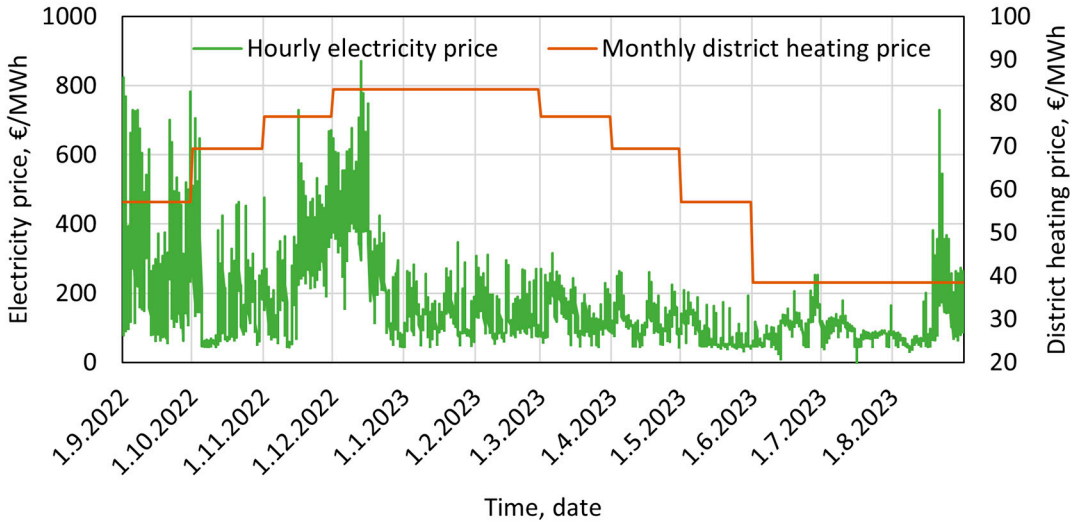

Figure 5. Hourly electricity price and monthly district heating price (including all taxes) in the first year with cost-effective control.

2.8. CO_2 Emissions

The CO_2 emissions from the energy use of the hybrid GSHP system were evaluated to investigate the environmental impacts of the control strategies. The CO_2 emissions were assessed for the electricity consumption and the district heating consumption for backup heating, respectively. For electricity consumption, a CO_2 emission factor of 33 $kgCO_2/MWh$ was used, taken from the average value in 2023 defined by Finnish Energy [32]. For the

district heating consumption, a CO_2 emission factor of 107.8 $kgCO_2/MWh$ was used, which is derived from the average value in 2023 from a local district heating provider.

2.9. Simulation Period and Weather Data

This study conducted two types of simulations: short-term and long-term. The short-term simulation period is 5.5 years, from March 2018 to August 2023. The simulation comprises two phases: the pre-calculation phase and the optimization phase. The pre-calculation phase was from March 2018 to August 2022 for calculating the thermal behavior of the ground. During this period, the hybrid heating and cooling system was operating with the design indoor heating and cooling setpoints and the GSHP-prioritized control strategy (see Section 2.5.1). There were no power limits applied to the GSHP and district heating. The optimization phase was from September 2022 to August 2023. In this period, the new indoor heating and cooling setpoints and the cost-effective control strategy (see Section 2.5.2) were used. The input hourly weather data for the short-term simulation were obtained from the weather stations of the Finnish Meteorological Institute in the vicinity of the studied building. During the short simulation period, the outdoor temperature varies between −23.9 °C and 32.4 °C, with an annual average ranging from 6.2 °C to 8.1 °C.

The long-term simulation period started in March 2018 and ended in February 2048. It also contains two phases: the pre-calculation phase and the optimization phase. The pre-calculation phase was the same as that in the short-term simulation, while the optimization phase was extended to February 2048. From March 2018 to August 2023, the input weather data remained consistent with that used in the short-term simulation. Subsequently, for the remainder of the simulation period, the input weather data were generated by cyclically duplicating the weather data clip between September 2022 and August 2023. The same method was used to generate the input data of real-time electricity and district heating prices.

2.10. Model Validation

The borehole model was validated in a prior study [27] within the validation period from March 2018 to February 2021. The results showed that the deviations of the borehole field inlet and outlet brine temperatures between the simulation and measurement are within 1 °C.

The combined model of building and hybrid GSHP system was validated in a separate study [33], spanning from July 2019 to June 2020. The results showed that the developed building model can simulate the monthly heating energy demand in the heating season, the monthly cooling energy demand in the cooling season, and the monthly DHW energy demand within a relative difference of 5%. The simulated ground thermal imbalance ratio, average hourly heat pump COP, GSHP heating energy ratio, and borehole free cooling energy ratio deviate from the measured values by 5%, respectively.

However, since the indoor air cooling setpoint was changed after August 2022, a new validation was carried out in this study for the simplified building model from September 2022 to August 2023. The simulated monthly energy demands for heating, cooling, and DHW are compared with the corresponding measured values in the next section. The measured data were obtained from the building automation system.

2.11. Description of Simulated Cases

The simulated cases are presented in Table 6. There are 14 cases designed for analysis. Cases 1 and 2 are designed to compare different control strategies. Case 1 is the reference case using the GSHP-prioritized control strategy in the optimization phase. In Case 2, the cost-effective control strategy is implemented, using a COP value of 4.2 and a control time horizon of 3 h, both derived from the real case. Based on Case 2, Cases 3 and 4 assess the effects of the maximum heating power of GSHP and district heating. In Case 3, the maximum district heating power is reduced to 1000 kW in the optimization phase (60% of the designed power). In Case 4, the maximum GSHP heating power is reduced to 632 kW

in the optimization phase (80% of the designed power at the rating conditions). Further analysis follows with Cases 4−9 for comparing different COP values for control. Finally, different control time horizons are explored in Cases 6 and 10−14.

Table 6. Descriptions of Cases 1−14.

Case	Control Strategy	Maximum Heat Pump Heating Power in the Optimization Phase, kW	Maximum District Heating Power in the Optimization Phase, kW	Heat Pump COP Value for Control (COP_{ctrl})	Control Time Horizon, h
Case 1 (ref)	GSHP-prioritized	790	1680	–	–
Case 2	Cost-effective	790	1680	4.2	3
Case 3	Cost-effective	790	1000	4.2	3
Case 4	Cost-effective	632	1000	4.2	3
Case 5	Cost-effective	632	1000	4.0	3
Case 6	Cost-effective	632	1000	3.8	3
Case 7	Cost-effective	632	1000	3.6	3
Case 8	Cost-effective	632	1000	3.4	3
Case 9	Cost-effective	632	1000	3.2	3
Case 10	Cost-effective	632	1000	3.8	1
Case 11	Cost-effective	632	1000	3.8	2
Case 12	Cost-effective	632	1000	3.8	4
Case 13	Cost-effective	632	1000	3.8	5
Case 14	Cost-effective	632	1000	3.8	6

3. Results

The results are presented in four sections. Section 3.1 analyzes the validation results of the building model. In Section 3.2, the effects of heating power limits of district heating and GSHP are investigated through a comparison of Cases 1–4. Then, Section 3.3 explores the effects of the heat pump COP_{ctrl} value using the results from Cases 1 and 4 to 9. Finally, Section 3.4 elaborates on the effects of the control time horizon based on the results from Cases 1, 6, and 10 to 14.

3.1. Building Model Validation

Figure 6 shows the monthly energy demand for heating, cooling, and DHW in the validation period from September 2022 to August 2023. The simulated values of monthly heating, cooling, and domestic hot water (DHW) energy are generated by IDA ICE 4.8. It can be seen that the simulated results closely match the measured data. The deviations between simulated and measured values remain within 5% for the monthly heating energy demand, 4% for the monthly cooling energy demand, and 4% for the monthly DHW energy demand, respectively. The annual heating, cooling, and DHW energy demands show deviations of 1%, 1%, and 2%, respectively.

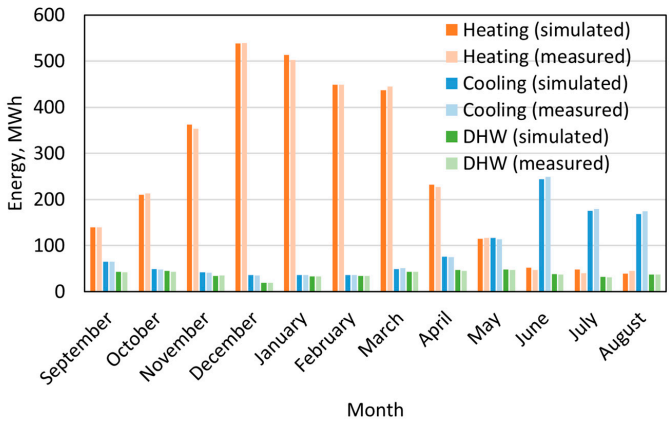

Figure 6. Measured and simulated monthly energy demand for heating, cooling, and DHW during the validation period.

3.2. Effects of Heating Power Limits

In Figure 7, the duration graphs of heating power in the first year with cost-effective control for Cases 1–4 are illustrated. Notably, as shown in Figure 7a, in Case 1 (reference case), the GSHP meets the base heating demand, and the district heating supplements during the peak heating demand period. The peak total heating power reaches 1530 kW, with a contribution of 797 kW from GSHP and 733 kW from the district heating, respectively. Figure 7b shows that in Case 2, the implementation of the new control strategy results in more usage of district heating. The peak total heating demand is even fully covered by district heating. In Case 3, a district heating power limit of 1000 kW leads to a marginal usage of GSHP during the peak heating demand period, as shown in Figure 7c. And a further restriction on the GSHP heating power in Case 4 causes more usage of district heating energy throughout the year compared to Case 3, as shown in Figure 7d.

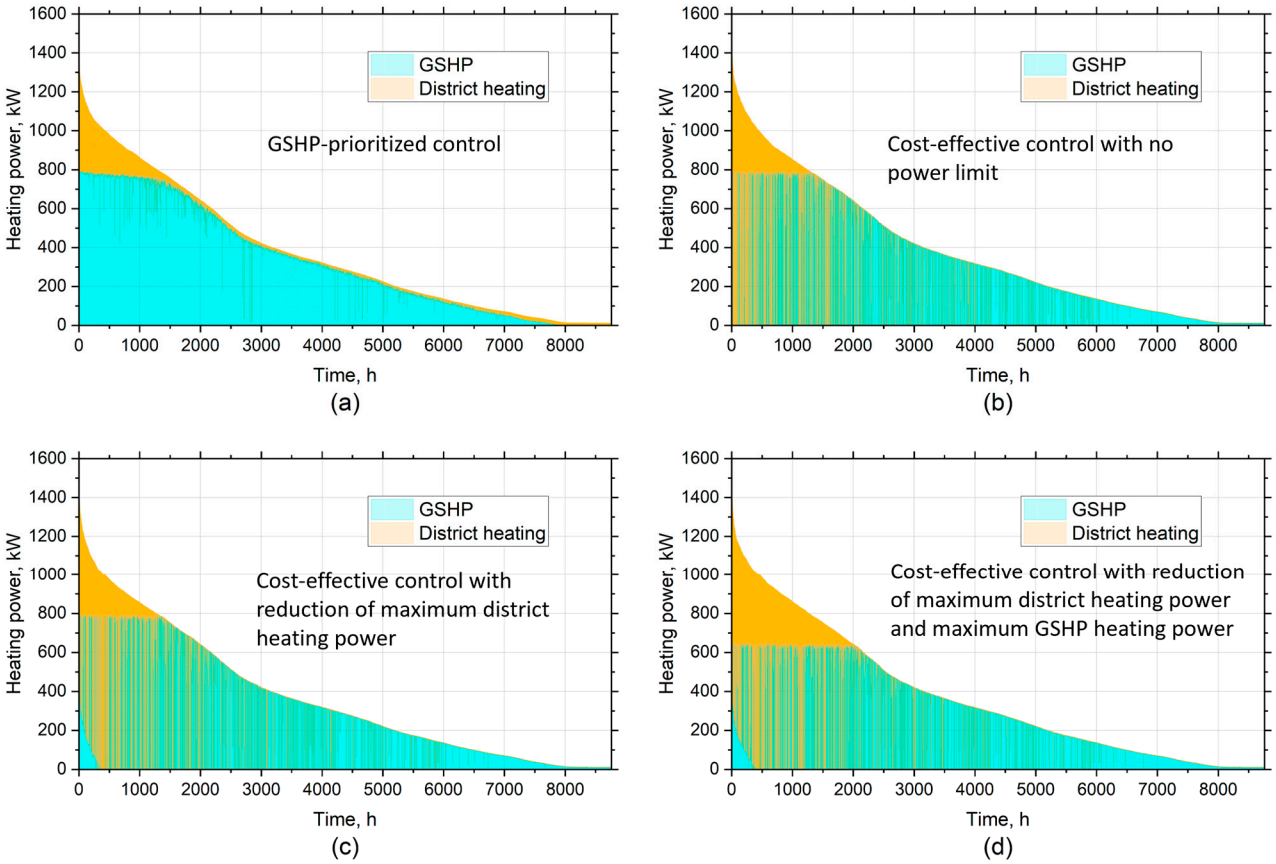

Figure 7. Duration graphs of heating power in the first year with cost-effective control: (**a**) Cases 1 (reference case), (**b**) Case 2, (**c**) Case 3, and (**d**) Case 4.

Table 7 shows the hybrid GSHP system performance in the first year with cost-effective control for Cases 1−4. Case 1 (the reference case) presents that the operational time of GSHP accounts for 85.3% of the year. The GSHP covers 89.7% of the annual total heating energy. This high reliance on the GSHP heating comes with a high risk of ground thermal imbalance, with a ground thermal imbalance ratio of 68.0%. The seasonal performance factor of the GSHP in Case 1 is 3.49. The comparison of Cases 1 and 2 shows that the cost-effective control reduces the operation time of GSHP. In Case 2, the GSHP operational time ratio is reduced to 78.7%, contributing to a decrease of 11.7 percentage points in the GSHP heating energy ratio compared to Case 1. The decreased usage of GSHP mitigates the ground thermal imbalance. The ground thermal imbalance ratio in Case 2 is 60.9%, reduced by 7.1 percentage points compared to Case 1. The lower thermal imbalance brings about a higher brine temperature in the heating season. Consequently, it contributes to a

1.3% higher seasonal performance factor in Case 2. In Case 3, a reduction of 40% in the maximum district heating power only causes an increase of 1.2 percentage points in the GSHP operational time ratio, which has a negligible impact on the GSHP heating energy ratio, the ground thermal imbalance ratio, and the seasonal performance factor. In Case 4, the GSHP operational time ratio remains the same as that in Case 3, while the GSHP heating energy ratio is decreased by 5.9 percentage points due to a reduction in the maximum GSHP heating power. Compared to Case 3, the ground thermal imbalance ratio is decreased by 3.1 percentage points, and thus, the seasonal performance factor is increased by 2.8%.

Table 7. Hybrid GSHP system performance for Cases 1−4 in the first year with cost-effective control.

Case	GSHP Operational Time Ratio (TR), %	GSHP Heating Energy Ratio (HR), %	Ground Thermal Imbalance Ratio (IR), %	Seasonal Performance Factor (SPF)
Case 1 (ref)	85.3	89.7	68.0	3.49
Case 2	78.7	78.0	60.9	3.54
Case 3	79.9	78.5	61.2	3.54
Case 4	79.9	72.7	58.1	3.64

Table 8 shows the energy costs in the first year with cost-effective control for Cases 1−4. Compared to Case 1, in Case 2, the cost-effective control does reduce the electricity energy cost. However, the increases in the district heating energy and power costs exceed the cost savings on the electricity energy cost. Therefore, the total energy cost in Case 2 is increased by 5.9% compared to Case 1. In Case 3, when the maximum district heating power is reduced by 40%, the increase in the district heating power cost is limited. Therefore, the cost-effective control brings cost savings to the hybrid GSHP system. The total energy cost in Case 3 is reduced by 2.9% compared to Case 1. In Case 4, when the maximum GSHP heating power is reduced by 20%, the total energy costs are reduced only by 1.9% compared to Case 1, which is mainly due to more district heating energy costs. The different outcomes from the district heating power limit (Cases 3) and GSHP power limit (Case 4) could be attributed to the contrasting shares of district heating in the peak heating power and annual total heating energy. Even though the district heating covers a large amount of the peak heating power (100% in Case 2), it only covers a minimal part of the total heating energy (22% in Case 2). Consequently, in Case 3, the district heating power limit contributes more to the reduction in district heating power cost, whereas in Case 4, the GSHP power limit results in a greater increase in the district heating energy cost instead.

Table 8. Energy costs for Cases 1−4 in the first year with cost-effective control.

Case	Cost, €/m^2					Rel.
	District Heating Energy	Electricity Energy	District Heating Power	Electricity Power	Total	
Case 1 (ref)	0.55	4.0	1.3	0.22	6.1	–
Case 2	1.2	2.7	2.3	0.22	6.4	5.9%
Case 3	1.2	2.7	1.7	0.22	5.9	−2.9%
Case 4	1.5	2.5	1.7	0.20	6.0	−1.9%

Table 9 shows the CO_2 emissions in the first year with cost-effective control for Cases 1−4. Compared to Case 1, the total CO_2 emissions increased by 55.9%, 53.2%, and 81.1% in Cases 2−4, respectively. Since the used CO_2 emission factor for district heating is two times higher than that for electricity, it becomes evident that the higher utilization of district heating will lead to increased CO_2 emissions in the cost-optimized cases.

Table 9. CO_2 emissions for Cases 1−4 in the first year with cost-effective control.

Case	CO_2 Emissions, Ton			Rel.
	Electricity	District Heating	Total	
Case 1 (ref)	30.6	37.3	67.8	–
Case 2	26.6	79.1	105.7	55.9%
Case 3	26.7	77.2	103.9	53.2%
Case 4	24.4	98.5	122.9	81.1%

Figure 8 illustrates the variation in the mean brine temperature over 30 years. Table 10 shows the minimum and maximum brine temperatures in the 1st year and the 30th year. It can be seen that in Case 1 with the GSHP-prioritized control strategy, the annual minimum brine temperature will drop below 0 °C in the 14th year and continue decreasing to −1.5 °C by the 30th year. Meanwhile, the annual maximum brine temperature will drop from 16.9 °C in the 1st year to 13.1 °C by the 30th year. In Cases 2 and 3, the cost-effective control mitigates the change in brine temperature. However, even with this strategy, the annual minimum brine temperature may still drop below 0 °C, reaching −0.8 °C by the 30th year. In Case 4, where the maximum GSHP heating power is limited, the annual minimum brine temperature in the 30th year can potentially reach 1.0 °C, indicating no freezing risk for the boreholes. Meanwhile, in Case 4, the annual maximum brine temperature in the 30th year is increased to 14.0 °C compared to Case 1.

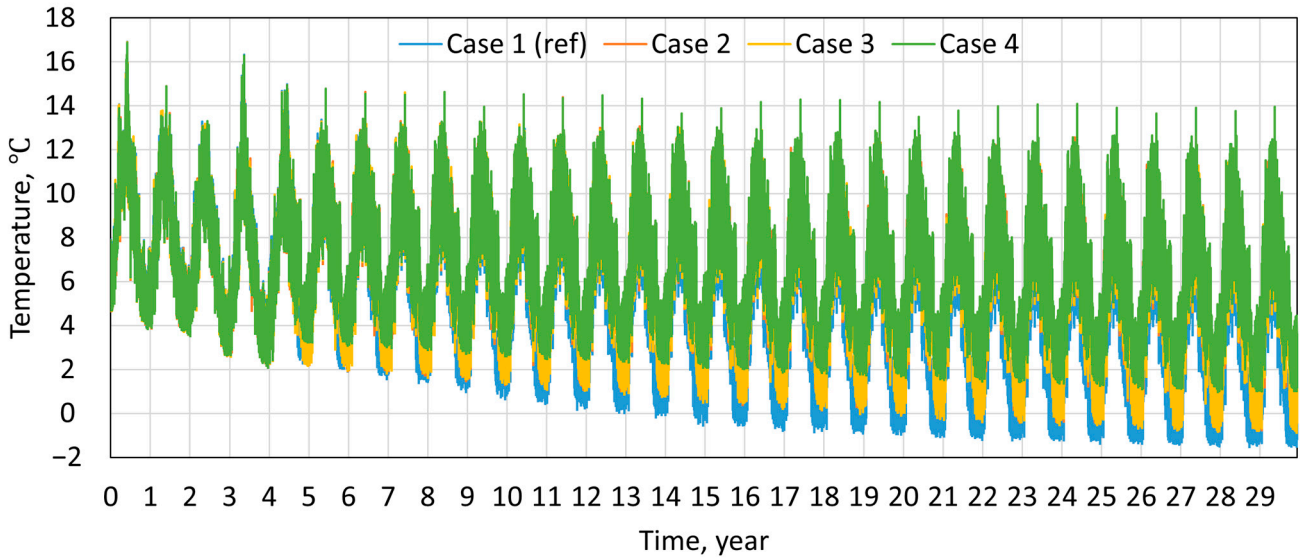

Figure 8. Mean brine temperature over 30 years.

Table 10. Mean brine temperature for Cases 1−4 in the 1st year and 30th year.

Case	1st Year		30th Year	
	$T_{f,min}$, °C	$T_{f,max}$, °C	$T_{f,min}$, °C	$T_{f,max}$, °C
Case 1 (ref)	4.0	16.9	−1.5	13.1
Case 2	3.9	16.9	−0.8	13.7
Case 3	3.9	16.9	−0.8	13.7
Case 4	3.9	16.9	1.0	14.0

3.3. Effects of Heat Pump COP Value for Control

Table 11 shows the hybrid GSHP system performance in the first year with cost-effective control for Cases 1 and 4−9. As the table shows, using a smaller COP_{ctrl} in the cost-effective control (see Equation (1)) results in a decreased operational time of GSHP.

When the COP_{ctrl} decreased from 4.2 to 3.2, the GSHP operational time ratio was reduced by 4.5 percentage points, leading to a decrease of 4.8 percentage points in the GSHP heating energy ratio and a reduction of 5.0 percentage points in the ground thermal imbalance ratio. However, the value of COP_{ctrl} has only a marginal effect on the seasonal performance factor of the GSHP.

Table 11. Hybrid GSHP system performance for Cases 1 and 4−9 in the first year with cost-effective control.

Case	COP_{ctrl}	GSHP Operational Time Ratio (TR), %	GSHP Heating Energy Ratio (HR), %	Ground Thermal Imbalance Ratio (IR), %	Seasonal Performance Factor (SPF)
Case 1 (ref)	–	85.3	89.7	68.0	3.49
Case 4	4.2	79.9	72.7	58.1	3.64
Case 5	4.0	79.2	71.9	57.5	3.64
Case 6	3.8	78.2	70.4	56.1	3.64
Case 7	3.6	77.2	69.2	55.2	3.65
Case 8	3.4	76.3	68.0	54.2	3.65
Case 9	3.2	75.4	66.9	53.1	3.65

Table 12 shows the energy costs in the first year with cost-effective control for Cases 1 and 4−9. As the usage time of GSHP is reduced with the decrease in COP_{ctrl}, the total electricity cost is reduced, while the total district heating cost increases accordingly. The total energy cost reaches its minimum value of 5.9 €/m^2 in Cases 5–7, reduced by 2.2% compared to the reference case. The minimum value appears when the COP_{ctrl} value ranges from 3.6 to 4.0, which is approximately the range between the seasonal performance factor and the COP at rated conditions. When the COP_{ctrl} value is away from this range, the total energy cost increases. However, it should be noted that the variations in the relative difference in total cost remain within 0.3% when COP_{ctrl} varies within the studied range (3.2–4.2).

Table 12. Energy costs for Cases 1 and 4−9 in the first year with cost-effective control.

Case	COP_{ctrl}	Cost, €/m^2					Rel.
		District Heating Energy	Electricity Energy	District Heating Power	Electricity Power	Total	
Case 1 (ref)	–	0.55	4.0	1.3	0.22	6.1	-
Case 4	4.2	1.5	2.5	1.7	0.20	6.0	−1.9%
Case 5	4.0	1.6	2.4	1.7	0.20	5.9	−2.2%
Case 6	3.8	1.7	2.3	1.7	0.20	5.9	−2.2%
Case 7	3.6	1.7	2.3	1.7	0.20	5.9	−2.2%
Case 8	3.4	1.8	2.2	1.7	0.20	6.0	−1.9%
Case 9	3.2	1.9	2.2	1.7	0.20	6.0	−1.9%

Table 13 shows the CO_2 emissions in the first year with cost-effective control for Cases 1 and 4−9. As previously stated, the used CO_2 emission factor for district heating is significantly higher than that for electricity. Therefore, when the COP_{ctrl} decreases, the total CO_2 emissions increase as more district heating is used. In Cases 5−7, where the total energy cost is minimized, the increase in the total CO_2 emissions ranges from 84.6% to 97.7%.

Table 13. CO_2 emissions for Cases 1 and 4−9 in the first year with cost-effective control.

Case	COP_{ctrl}	CO_2 Emissions, Ton			Rel.
		Electricity	District Heating	Total	
Case 1 (ref)	–	30.6	37.3	67.8	–
Case 4	4.2	24.4	98.5	122.9	81.1%
Case 5	4.0	24.1	101.1	125.2	84.6%
Case 6	3.8	23.7	106.3	130.0	91.6%
Case 7	3.6	23.4	110.8	134.1	97.7%
Case 8	3.4	23.0	115.5	138.5	104.2%
Case 9	3.2	22.7	119.0	141.7	108.9%

Table 14 gives the mean brine temperature in the 1st year and 30th year for Cases 1 and 4−9. The annual minimum brine temperature in the 30th year is evidently higher for smaller COP_{ctrl} values as the usage of GSHP is reduced. In Cases 5−7, where the total energy cost is minimized, the annual minimum brine temperature in the 30th year ranges between 1.1 °C and 1.5 °C. However, the variation in COP_{ctrl} insignificantly affects the annual maximum brine temperature.

Table 14. Mean brine temperature for Cases 1 and 4−9 in the 1st year and 30th year.

Case	COP_{ctrl}	1st Year		30th Year	
		$T_{f,min}$, °C	$T_{f,max}$, °C	$T_{f,min}$, °C	$T_{f,max}$, °C
Case 1 (ref)	–	4.0	16.9	−1.5	13.1
Case 4	4.2	3.9	16.9	1.0	14.0
Case 5	4.0	3.9	16.9	1.1	14.0
Case 6	3.8	3.9	16.9	1.3	14.1
Case 7	3.6	3.9	16.9	1.5	14.0
Case 8	3.4	3.9	16.9	1.6	14.1
Case 9	3.2	3.9	16.9	1.7	14.0

3.4. Effects of Control Time Horizon

Table 15 presents the hybrid GSHP system performance for Cases 1, 6, and 10−14 in the first year with cost-effective control. It seems that the control time horizon has marginal effects on the usage of GSHP. The GSHP operational time ratio is reduced by only 0.4 percentage points when the control time horizon is increased from 1 h to 6 h. The marginal effects are also reflected in the GSHP heating energy ratio, ground thermal imbalance, and the seasonal performance factor.

Table 15. Hybrid GSHP system performance for Cases 1, 6, and 10−14 in the first year with cost-effective control.

Case	Control Time Horizon, h	GSHP Operational time Ratio (TR), %	GSHP Heating Energy Ratio (HR), %	Ground Thermal Imbalance Ratio (IR), %	Seasonal Performance Factor (SPF)
Case 1 (ref)	–	85.3	89.7	68.0	3.49
Case 10	1	78.6	70.3	56.0	3.64
Case 11	2	78.3	70.4	56.3	3.64
Case 6	3	78.2	70.4	56.1	3.64
Case 12	4	78.4	70.6	56.5	3.64
Case 13	5	78.3	70.8	56.6	3.64
Case 14	6	78.2	70.9	56.8	3.64

Tables 16 and 17 present energy costs and CO_2 emissions for Cases 1, 6, and 10−14, respectively, in the first year with cost-effective control. Table 18 shows the mean brine

temperature for Cases 1, 6, and 10−14 in the 1st year and 30th year. As the control time horizon has a minimal impact on the usage of GSHP, the consequent effects on the energy cost and CO_2 emissions in the first year with cost-effective control are insignificant, as well as the effect on the long-term behavior of brine temperature.

Table 16. Energy costs in the first year with cost-effective control for Cases 1, 6, and 10−14 in the first year with cost-effective control.

Case	Control Time Horizon, h	Cost, €/m^2					Rel.
		District Heating Energy	Electricity Energy	District Heating Power	Electricity Power	Total	
Case 1 (ref)	–	0.55	4.0	1.3	0.22	6.1	–
Case 10	1	1.7	2.3	1.7	0.20	5.9	−2.2%
Case 11	2	1.7	2.3	1.7	0.20	5.9	−2.1%
Case 6	3	1.7	2.3	1.7	0.20	5.9	−2.2%
Case 12	4	1.7	2.3	1.7	0.20	5.9	−2.1%
Case 13	5	1.6	2.4	1.7	0.20	5.9	−2.1%
Case 14	6	1.6	2.4	1.7	0.20	5.9	−2.1%

Table 17. CO_2 emissions for Cases 1, 6, and 10−14 in the first year with cost-effective control.

Case	Control Time Horizon, h	CO_2 Emissions, Ton			Rel.
		Electricity	District Heating	Total	
Case 1 (ref)	–	30.6	37.3	67.8	–
Case 10	1	23.7	106.8	130.5	92.4%
Case 11	2	23.7	106.4	130.1	91.8%
Case 6	3	23.7	106.3	130.0	91.6%
Case 12	4	23.8	106.0	129.7	91.2%
Case 13	5	23.8	105.1	128.9	90.0%
Case 14	6	23.8	104.7	128.6	89.5%

Table 18. Mean brine temperature for Cases 1, 6, and 10−14 in the 1st year and 30th year.

Case	Control Time Horizon, h	1st Year		30th Year	
		$T_{f,min}$, °C	$T_{f,max}$, °C	$T_{f,min}$, °C	$T_{f,max}$, °C
Case 1 (ref)	–	4.0	16.9	−1.5	13.1
Case 10	1	3.9	16.9	1.3	13.9
Case 11	2	3.9	16.9	1.3	13.9
Case 6	3	3.9	16.9	1.3	14.1
Case 12	4	3.9	16.9	1.2	14.0
Case 13	5	3.9	16.9	1.3	13.9
Case 14	6	3.9	16.9	1.2	13.9

The insignificant effects of the control time horizon could be due to the magnitude and frequency of energy price changes. In this study, the district heating price varies monthly, which means the decision for selecting the primary heating source is determined mainly by the behavior of electricity price. If the electricity price varies within a small range and does not generate a significant hourly heating price difference $\left(\frac{c_e(\tau)}{COP_{ctrl}} - \frac{c_d(\tau)}{\eta_{dh}}\right)$ for a certain period, the variation in the control time horizon may not impact the usage time of GSHP and consequently will have marginal effects on other results.

4. Discussion

This study used rule-based control instead of model-based control to reduce the energy cost of the hybrid GSHP system. Even though, compared to rule-based control methods, some model-based control methods may offer better results within variable constraints,

rule-based control is still preferred in actual cases due to its considerable simplicity and wide applicability. It may continue to be the dominant control method for the next two decades [17]. The study provides insights into the feasibility of cost savings through the developed rule-based control strategy. However, conducting comparable studies between rule-based and model-based control methods would be interesting for future work.

The control parameters were investigated within specific value ranges. For power limits, this study examined a 40% decrease in district heating power and a 20% decrease in heat pump heating power. Additionally, the values of COP_{ctrl} and the control time horizon were explored within certain ranges. The simulation results clearly demonstrated the effects of these parameters on the system's annual energy cost, CO_2 emissions, and long-term borehole heat exchanger performance. However, future studies could explore other values of these control parameters to further understand their impacts.

The control parameters should be determined to prioritize the long-term operational safety of the hybrid GSHP system, followed by the minimization of energy costs. The studied GSHP system will still face a risk of borehole freezing over the next 25 years, even with the cost-effective control. Therefore, reducing ground thermal imbalance is a top priority. Based on the parameter analysis, limiting the power of district heating can reliably reduce the annual total energy cost without significantly affecting the ground thermal imbalance. However, there is a conflict when it comes to deciding the power limit on GSHP and the value of COP_{ctrl}. The study recommends first limiting the GSHP power to ensure the borehole system remains nonfreezing and then selecting an appropriate value for COP_{ctrl}. The optimal COP_{ctrl} value for cost savings ranges from 3.6 to 4.0, which is approximately between the seasonal performance factor and the COP at rated conditions. Practically, it is easier to set the COP value at rated conditions as COP_{ctrl}. However, if measurement data for the GSHP are available, using the seasonal performance factor as COP_{ctrl} is possible since the smaller value of COP_{ctrl} can further mitigate ground thermal imbalance and reduce long-term brine temperature variation.

A good question is whether to keep the ground fully balanced during the whole lifetime. The developed cost-effective control strategy cannot consider the constraint of zero thermal imbalance. By reducing the power of GSHP and adjusting the COP_{ctrl}, the borehole system was maintained under nonfreezing conditions for the next 25 years. However, the ground thermal imbalance was not eliminated. The brine temperature would still drop year by year. The decrease in the brine temperature may affect both GSHP heating and free cooling performances and thus influence the long-term energy cost. Nevertheless, the energy cost can be influenced by factors such as future climate changes, energy escalation rates, and real interest rates. In the future, it would be interesting to carry out detailed research regarding the effect of ground thermal balance on the long-term energy cost.

To maintain ground thermal balance, using solar energy to charge the ground could be another possibility. Installing solar collectors involves additional investment, which requires a detailed life cycle assessment. Additionally, it will further complicate the control of the hybrid GSHP system. The feasibility and benefits of this solar-assisted GSHP system could be investigated in future work.

The annual energy cost savings through the cost-effective control could be dependent on real-time energy prices. The magnitude and frequency of energy price changes could affect cost savings. This study uses hourly electricity prices and monthly district heating prices from September 2022 to August 2023. The annual cost savings through the cost-effective control was visible. However, in years with significantly lower electricity prices or higher district heating prices, the cost-effective control may not be more beneficial than the GSHP-prioritized control. In addition, the study found that the effects of the control time horizon were marginal. However, in scenarios with more frequent and significant price changes, the impact of adjusting the control time horizon could become more pronounced. In the future, sensitive analysis could be carried out to test the cost-effective control strategy under various energy price scenarios and different energy tariffs.

The proposed cost-effective control could not lead to the preferred lowest CO_2 emissions under the condition of current CO_2 emission factors. In Finland, district heating currently carries higher CO_2 emissions compared to electricity, primarily due to its higher reliance on fossil fuels. However, this trend will be changed in the future when more renewable energy sources are integrated into district heating production to realize the carbon-neutral target by 2035 [34]. More detailed CO_2 emission analyses for different decarbonization scenarios could be considered in future work.

For building owners, implementing the cost-effective control strategy in a hybrid GSHP system requires advanced metering and automation. This involves the installation of energy meters and the programming of control algorithms. Additionally, experts are needed to analyze the performance of both the building and the complex hybrid GSHP system, providing guidance on setting key control parameters. For example, to determine the power limits, it is essential to know how much district heating and GSHP power can be safely restricted without compromising peak heating power supply and risking indoor thermal comfort. Therefore, a comprehensive analysis of heating demand and the indoor thermal environment is necessary before making decisions. A straightforward solution could be to purchase corresponding energy services from an energy company. This will ensure reliable and professional energy management, maintenance, and monitoring services.

5. Conclusions

This study presented a cost-effective control strategy for reducing energy costs in a hybrid GSHP system combined with district heating from the perspective of building owners. The hybrid GSHP system was modeled and simulated by IDA ICE 4.8. The effect of heating power limits of GSHP/district heating, the heat pump COP value for control (COP_{ctrl}), and the control time horizon in the cost-effective control strategy were investigated across different cases. The contributions of this study are summarized as follows:

- The power limit on district heating is essential for reducing the energy cost through cost-effective control. Compared to the GSHP-prioritized control, the cost-effective control strategy can reduce the costs for used electricity and district heating energy, but it causes more increase in the district heating power cost. However, a power limit on district heating can assist the cost-effective control strategy in reducing the annual total energy cost. The result showed that the cost-effective control with a 60% district heating power limit can reduce the annual total energy cost by 2.9%.
- The power limit on GSHP is necessary for ensuring the system's long-term operation safety. The cost-effective control strategy can mitigate the ground thermal imbalance and improve the GSHP seasonal performance factor, but the control cannot ensure the hybrid GSHP system operates safely for long term. Thus, the power limit on the heat pump should be applied to the hybrid GSHP system, even though it impairs the cost savings. The result showed that the cost-effective control with a 60% power limit on district heating and an 80% power limit on GSHP heating can maintain the mean brine temperature above 1 °C for the next 25 years and achieve a 1.9% reduction in the annual total energy cost.
- The COP_{ctrl} value needs to be selected carefully for the cost-effective control. There existed an optimal range of COP_{ctrl} value to achieve higher energy cost savings. The annual total energy cost was minimized when the COP_{ctrl} value ranged from 3.6 to 4.0, which is approximately the range between the seasonal performance factor and the COP at rated condition. However, using the smaller COP_{ctrl} value can mitigate the ground thermal imbalance and reduce the long-term brine temperature variation. Therefore, the COP_{ctrl} value of 3.6, is recommended for the studied hybrid GSHP system. Finally, the annual total energy cost was reduced by 2.2% with the recommended COP_{ctrl} and power limits on district heating and GSHP.
- The control time horizon had a marginal effect on the annual total energy cost and long-term brine temperature behavior under the used energy price scenario.

- The cost-effective control strategy caused more CO_2 emissions due to higher CO_2 emissions from district heating. However, the decarbonization of the energy product may make this control strategy more environmentally friendly in the future.
- Implementing the cost-effective control in the actual hybrid GSHP system could involve reducing the maximum district heating power and maximum GSHP heating power, as well as setting an appropriate COP_{ctrl} value. It is advisable to choose the value near the seasonal performance factor of GSHP.

Author Contributions: Conceptualization, T.X., J.J. and R.K.; methodology, T.X., J.J. and R.K.; software, T.X., J.J. and R.K.; validation, T.X., J.J. and R.K.; formal analysis, T.X.; investigation, T.X.; resources, J.J. and R.K.; data curation, J.J. and R.K.; writing—original draft preparation, T.X.; writing—review and editing, J.J. and R.K.; visualization, T.X.; supervision, J.J. and R.K.; project administration, R.K.; funding acquisition, R.K. and J.J. All authors have read and agreed to the published version of the manuscript.

Funding: This study was financially supported by the China Scholarship Council (No. 202006370019) and Aalto University Campus & Real Estate (No. 411086). Moreover, funding was provided by the B2RECoM project (No. 10784/31/2022), supported by Business Finland.

Data Availability Statement: Data are contained within the article.

Acknowledgments: The authors would like to thank ACRE for providing the technical information and measured data. Additionally, the authors would like to especially thank Tuomas Keyriläinen for the expert support related to the building automation system and the Geological Survey of Finland (GTK) for the useful data regarding simulation.

Conflicts of Interest: The authors declare no conflicts of interest.

References

1. Tracking Buildings. 2022. Available online: https://www.iea.org/energy-system/buildings (accessed on 11 January 2024).
2. United Nations Environment Programme. *2022 Global Status Report for Buildings and Construction: Towards a Zero-Emission, Efficient and Resilient Buildings and Construction Sector*; United Nations Environment Programme: Nairobi, Kenya, 2022; Volume 224.
3. Wang, P.; Wang, Y.; Gao, W.; Xu, T.; Wei, X.; Shi, C.; Qi, Z.; Bai, L. Uncovering the Efficiency and Performance of Ground-Source Heat Pumps in Cold Regions: A Case Study of a Public Building in Northern China. *Buildings* **2023**, *13*, 1564. [CrossRef]
4. Menegazzo, D.; Lombardo, G.; Bobbo, S.; De Carli, M.; Fedele, L. State of the Art, Perspective and Obstacles of Ground-Source Heat Pump Technology in the European Building Sector: A Review. *Energies* **2022**, *15*, 2685. [CrossRef]
5. Majuri, P. Technologies and environmental impacts of ground heat exchangers in Finland. *Geothermics* **2018**, *73*, 124–132. [CrossRef]
6. SULPU. Available online: https://www.sulpu.fi/english/ (accessed on 11 January 2024).
7. Peel, M.C.; Finlayson, B.L.; McMahon, T.A. Updated world map of the Köppen-Geiger climate classification. *Hydrol. Earth Syst. Sci.* **2007**, *11*, 1633–1644. [CrossRef]
8. Nordell, B.; Ahlström, A.-K. Freezing Problems in Borehole Heat Exchangers. In *Therm Energy Storage Sustain Energy Consum*; Springer: Berlin/Heidelberg, Germany, 2007; pp. 193–203. [CrossRef]
9. Ahmadfard, M.; Bernier, M. A review of vertical ground heat exchanger sizing tools including an inter-model comparison. *Renew. Sustain. Energy Rev.* **2019**, *110*, 247–265. [CrossRef]
10. Spitler, J.D.; Bernier, M. Vertical borehole ground heat exchanger design methods. In *Advances in Ground-Source Heat Pump Systems*; WoodHead Publishing: Amsterdam, The Netherlands, 2016. [CrossRef]
11. Atam, E.; Helsen, L. Ground-coupled heat pumps: Part 2-Literature review and research challenges in optimal design. *Renew. Sustain. Energy Rev.* **2016**, *54*, 1668–1684. [CrossRef]
12. Xu, L.; Pu, L.; Zhang, S.; Li, Y. Hybrid ground source heat pump system for overcoming soil thermal imbalance: A review. *Sustain. Energy Technol. Assess.* **2021**, *44*, 101098. [CrossRef]
13. Yang, R.; Wang, L. Efficient control of a solar assisted ground-source heat pump system based on evaluation of building thermal load demand. In Proceedings of the 2012 North American Power Symposium NAPS, Champaign, IL, USA, 9–11 October 2012; pp. 1–6. [CrossRef]
14. Dai, L.; Li, S.; DuanMu, L.; Li, X.; Shang, Y.; Dong, M. Experimental performance analysis of a solar assisted ground source heat pump system under different heating operation modes. *Appl. Therm. Eng.* **2015**, *75*, 325–333. [CrossRef]
15. Emmi, G.; Zarrella, A.; De Carli, M.; Galgaro, A. An analysis of solar assisted ground source heat pumps in cold climates. *Energy Convers. Manag.* **2015**, *106*, 660–675. [CrossRef]
16. Reda, F. Long term performance of different SAGSHP solutions for residential energy supply in Finland. *Appl. Energy* **2015**, *144*, 31–50. [CrossRef]

17. Atam, E.; Helsen, L. Ground-coupled heat pumps: Part 1-Literature review and research challenges in modeling and optimal control. *Renew. Sustain. Energy Rev.* **2016**, *54*, 1653–1667. [CrossRef]
18. Atam, E.; Patteeuw, D.; Antonov, S.P.; Helsen, L. Optimal Control Approaches for Analysis of Energy Use Minimization of Hybrid Ground-Coupled Heat Pump Systems. *IEEE Trans. Control Syst. Technol.* **2016**, *24*, 525–540. [CrossRef]
19. Puttige, A.R.; Andersson, S.; Östin, R.; Olofsson, T. Modeling and optimization of hybrid ground source heat pump with district heating and cooling. *Energy Build.* **2022**, *264*, 112065. [CrossRef]
20. Verhelst, C. Model Predictive Control of Ground Coupled Heat Pump Systems for Office Buildings. Ph.D. Thesis, KU Leuven, Leuven, Belgium, 2012. Available online: https://lirias.kuleuven.be/retrieve/183602 (accessed on 14 January 2024).
21. Weeratunge, H.; Narsilio, G.; de Hoog, J.; Dunstall, S.; Halgamuge, S. Model predictive control for a solar assisted ground source heat pump system. *Energy* **2018**, *152*, 974–984. [CrossRef]
22. Atam, E.; Helsen, L. A convex approach to a class of non-convex building HVAC control problems: Illustration by two case studies. *Energy Build.* **2015**, *93*, 269–281. [CrossRef]
23. Cupeiro Figueroa, I.; Picard, D.; Helsen, L. Short-term modeling of hybrid geothermal systems for Model Predictive Control. *Energy Build.* **2020**, *215*, 109884. [CrossRef]
24. Gustafsson, S.I.; Rönnqvist, M. Optimal heating of large block of flats. *Energy Build.* **2008**, *40*, 1699–1708. [CrossRef]
25. Sahlin, P. Modeling and Simulation Methods for Modular Continuous Systems in Buildings. Ph.D. Thesis, Royal Institute of Technology, Stockholm, Sweden, 1996.
26. Simulation, E. *Validation of IDA Indoor Climate and Energy 4.0 Build 4 with Respect to ANSI/ASHRAE Standard 140-2004*; Simulation Technology Group: Solna, Sweden, 2010.
27. Xue, T.; Jokisalo, J.; Kosonen, R.; Vuolle, M.; Marongiu, F.; Vallin, S.; Leppäharju, N.; Arola, T. Experimental evaluation of IDA ICE and COMSOL models for an asymmetric borehole thermal energy storage field in Nordic climate. *Appl. Therm. Eng.* **2022**, *217*, 119261. [CrossRef]
28. Ministry of Environment. *Decree (1010/2017) on the Energy Performance of the New Building*; Ministry of Environment: Helsinki, Finland, 2017. Available online: https://ym.fi/en/the-national-building-code-of-finland (accessed on 22 May 2024).
29. Niemelä, T.; Vuolle, M.; Kosonen, R.; Jokisalo, J.; Salmi, W.; Nisula, M. Dynamic simulation methods of heat pump systems as a part of dynamic energy simulation of buildings. In Proceedings of the 3rd IBPSA-England Conference BSO 2016, Newcastle, UK, 12–14 September 2016.
30. Alimohammadisagvand, B.; Jokisalo, J.; Kilpeläinen, S.; Ali, M.; Sirén, K. Cost-optimal thermal energy storage system for a residential building with heat pump heating and demand response control. *Appl. Energy* **2016**, *174*, 275–287. [CrossRef]
31. Nord Pool. Market Data. 2023. Available online: https://www.nordpoolgroup.com/en/Market-data1/Dayahead/Area-Prices/FI/Hourly/?view=table (accessed on 11 January 2024).
32. Finnish Energy. Energy Year 2023—Electricity. Available online: https://energia.fi/en/statistics/statistics-on-electricity/ (accessed on 20 January 2024).
33. Xue, T.; Jokisalo, J.; Kosonen, R. Design of High-Performing Hybrid Ground Source Heat Pump. *Buildings* **2023**, *13*, 1825. [CrossRef]
34. Riku, H.; Petteri, K.; Markku, K.; Bettina, L.; Hirvonen, P. *Carbon Neutral Finland 2035—National Climate and Energy Strategy*; Ministry of Economic Affairs and Employment of Finland: Helsinki, Finland, 2022.